

NUMERICAL STUDY OF DROPLET EVAPORATION

by

RITUL GANDHI

Presented to the Faculty of the Graduate School of
The University of Texas at Arlington in Partial Fulfillment
of the Requirements
for the Degree of

MASTER OF SCIENCE IN MECHANICAL ENGINEERING

THE UNIVERSITY OF TEXAS AT ARLINGTON

FALL 2017

Copyright © by Ritul Gandhi 2017

All Rights Reserved



Acknowledgements

I would like to dedicate this thesis to my parents. I am extremely grateful to my mother for supporting me; having faith in me even in the times when I was not confident in myself. My father for being an inspiration and supporting me throughout my journey from child to reaching this stage.

I would like to express my deepest gratitude to Dr. Hyejin Moon for providing me this research opportunity and allowed me to be a member of Integrated Micro Nanofluidics Lab (IMNfL). I am thankful for her guidance and being an inspiration throughout my research journey, she taught me the way of thinking and analyzing which helped me evolve continuously.

I am thankful to Dr. Miguel Amaya and Dr. Donghyun Shin for being a part of my defense committee and sharing their valuable feedback.

A very special thanks to MunMun Nahar and Viraj Sabane for helping me to get acquainted with COMSOL Multiphysics software. They helped me understand how to convert physical conditions into numerical ones which helped me to overcome challenges in COMSOL Multiphysics. I thank Matin Torabinia who helped me in validating my numerical simulation with the experiment. I am grateful to Arvind Venkatesan, for his support and being a mentor to me throughout this journey.

Lastly, I would like to express my vote of appreciation to my roommates and friends for supporting and encouraging me to accomplish this task.

December 6, 2017

Abstract

NUMERICAL STUDY OF DROPLET EVAPORATION

Ritul Gandhi, MS

The University of Texas at Arlington, 2017

Supervising Professor: Hyejin Moon

Droplet evaporation plays a vital role in various engineering fields such as air/fuel premixing, inkjet printing and many more. The high rate of power dissipation from the integrated circuits and chips of electronic devices creates a need for cooling it to achieve their optimal functionality. The high rate of cooling can be achieved by thin film evaporation of water by phase change as compared to the air cooling methods. Therefore, the study of droplet evaporation is necessary to understand the underlying physics and effects of different parameters on cooling performance.

Numerical study of droplet evaporation has been done by using the level set and arbitrary Lagrangian-Eulerian moving mesh method in COMSOL. These methods are used to track the shrinking liquid-gas interface because of phase change. The changes in the surface tension due to temperature gradient caused by the phase change induces Marangoni convection which influences evaporation. Investigation of the transient droplet evaporation is done wherein the radius of the droplet is pinned and the effect of Marangoni convection on the average droplet temperature is studied for the pure diffusion case. The model developed in this study can easily be extended to study contact line dynamics during droplet evaporation.

Table of Contents

Acknowledgements	iii
Abstract	iv
List of Illustrations	vii
List of Tables	ix
Chapter 1 INTRODUCTION.....	10
1.1 Motivation	10
1.2 Droplet Evaporation.....	10
1.3 Marangoni Convection (MA).....	13
1.4 Governing Equations	15
Chapter 2 INTERFACE TRACKING METHOD	17
2.1 Introduction	17
2.2 Level-set method (LS)	17
2.3 Arbitrary Lagrangian Eulerian moving mesh (ALE).....	19
Chapter 3 NUMERICAL STUDY	23
3.1 Introduction	23
3.2 Modelling	23
3.3 Assumptions	24
3.4 Pure diffusion model using Level-set method	24
3.4.1 Transport of diluted species (Air & water)	24
3.4.2 Laminar flow	26
3.4.3 Heat transfer in fluids	26
3.4.4 Multiphysics coupling	27
3.4.5 Results.....	28
3.4.6 Conclusion.....	30

3.5 Pure diffusion model using ALE moving mesh without Marangoni convection.....	30
3.5.1 Laminar two-phase flow with moving mesh	31
3.5.2 Transport of diluted species	32
3.5.3 Heat transfer in fluids	33
3.5.4 Meshing	34
3.5.5 Results.....	34
3.6 Pure diffusion model using ALE moving mesh with Marangoni convection.....	37
3.6.1 Results.....	37
3.7 Comparison of pure diffusion model with and without Marangoni convection.....	39
3.7.1 Summary	41
Chapter 4 EXPERIMENTAL VALIDATION	42
4.1 Introduction	42
4.2 Image processing	43
Chapter 5 DROPLET EVAPORATION ON HEATED SUBSTRATE	46
5.1 Introduction	46
5.2 Results.....	46
Chapter 6 FUTURE WORK	49
References	51
Biographical Information	53

List of Illustrations

Figure 1.1 Physics of evaporation.....	11
Figure 1.2 Plot of surface tension v/s temperature	13
Figure 1.3 Marangoni convection in sessile droplet.....	14
Figure 2.1 Evolving front in Level-set method.....	17
Figure 2.2 ALE moving mesh method.....	20
Figure 3.1 BC for transport of diluted species in air domain.....	25
Figure 3.2 B.C for transport of diluted species for water domain.	26
Figure 3.3 Physics coupling and calculation steps.	27
Figure 3.4 Volume fraction of fluid with time.	28
Figure 3.5 Concentration at the interface with time.	29
Figure 3.6 Average temperature of the bulk liquid.....	29
Figure 3.7 B.C for laminar flow	31
Figure 3.8 B.C. for transport of diluted species.	33
Figure 3.9 B.C. for heat transfer in fluids.	34
Figure 3.10 2D Meshing using free triangular elements.....	34
Figure 3.11 Concentration across the interface with time.....	35
Figure 3.12 Plot for the concentration (without MA).	35
Figure 3.13 Average temperature of the water droplet.....	36
Figure 3.14 Temperature of the water droplet (without MA).....	37
Figure 3.15 Plot of average temperature with and without MA.....	39
Figure 3.16 Temperature at the interface with and without MA.....	40
Figure 3.17 Evaporation rate of droplet with and without MA.....	41
Figure 4.1 Plot of droplet height.....	42
Figure 4.2 Droplet measurements taken using image processing.	44

Figure 4.3 Numerical model in COMSOL Multiphysics.....	45
Figure 5.1 Temperature condition at the liquid-solid interface.....	46
Figure 5.2 Concentration at the interface with time.	47
Figure 5.3 Plot of average droplet temperature with time.....	47
Figure 5.4 Plot of average mass flux across the interface with time.	48
Figure 6.1 Division of the extended droplet meniscus.	50

List of Tables

Table 1 Velocity and temperature profile of droplet (with MA).....	38
Table 2 Droplet evaporation at various time instances.....	43

Chapter 1

INTRODUCTION

1.1 Motivation

The advancement in the technology has led to the complexity of the electronic devices. The technological advancement in the fabrication techniques has made possible to increase the density of transistors, leading to miniaturization of electronic devices. These transistors are made up of silicon, they dissipate heat during their operation and to achieve optimal performance there arises a need to cool them down. The conventional ways of air cooling are irrelevant at such small sizes. Hence, to achieve more amount of thermal efficiency water cooling methods are adopted over air cooling. Thus, there arises the need to study the evaporation of water droplet and the underlying physics of the same.

1.2 Droplet Evaporation

Evaporation is a purely diffusive process. The evaporation rate is proportional to the difference between the vapor pressure of the saturated free surface and that of the overlying air. The high energy molecules on the free surface escape to the atmosphere reducing the average kinetic energy of the remaining molecules which results in a temperature drop of the bulk liquid. The average number of molecules leaving the free surface reduces with the time as the difference in the pressure of the saturated layer and ambient air decreases which is shown in the figure. [1]

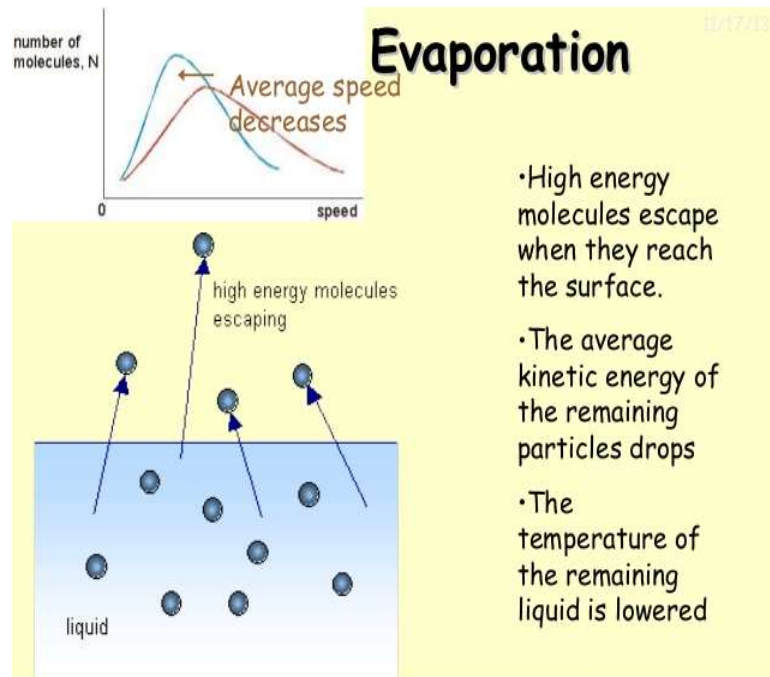


Figure 1.1 Physics of evaporation

The evaporation rate can be expressed as:

$$E \propto (P_{sat} - P_{air}) \quad (1)$$

Where,

E = evaporation rate;

P_{sat}, P_{air} = Saturated vapor pressure at the interface and overlying air respectively.

If we consider that water vapor acts as an ideal gas, then we can express the vapor pressure in terms of the concentration by using the ideal gas equation:

$$P \times V = m \times R \times T \quad (2)$$

$$\frac{m}{V} = \frac{P}{R \times T} ; \quad C = \frac{P}{R \times T} \quad (3)$$

where, C is the concentration expressed in mol/m^3 .

Now we can say that evaporation rate is proportional to the concentration gradient due to the saturated concentration at the interface and the concentration of the ambient air. If we do not consider the effects caused due to the external air flow or forced convection in our system, then the model can be termed as purely diffusive as it only depends on the concentration gradient such model is called *Pure Diffusion model*.

As there is a reduction in the temperature we can use evaporation for cooling purposes also. If we relate the above process of evaporation to a liquid droplet having small volumes in microliters then, there will be mainly three stages of droplet evaporation: (1) In the first stage, there will be the diminishing of the contact angle with the pinned contact line till 70% of the volume is evaporated. (2) For the next 25-27% volume, there will be constant contact angle with receding contact line. (3) Remaining 5-3% will have mix mode in which the reduction in contact angle as well as contact area will take place simultaneously. The phenomenon that takes place during the evaporation which consists of the following: (1) There will be a change of phase from liquid water to vapor form at the liquid-gas interface. (2) The saturated vapor at the interface will transfer into the atmosphere due to the concentration gradient. (3) As the mass loss is happening during the evaporation the interface will evolve continuously with the time i.e. it will shrink in a downward direction. (4) The stresses at the interface will change causing an internal convection inside the bulk fluid. (5) The mass loss at the liquid-gas interface will take away the latent heat of vaporization with it eventually decreasing the temperature at the interface which will cool down the underlying substrate due to the heat transfer taking place between the substrate and the droplet. All the above-mentioned phenomenon takes place simultaneously with time and eventually the drop will get evaporated in the air.

1.3 Marangoni Convection (MA)

It is an interfacial phenomenon which is induced by the surface tension gradient.

Temperature, concentration of the solute and electric field can affect the surface tension.

The equation uniting all the terms is as below: [2]

$$\partial\sigma = \frac{\partial\sigma}{\partial T}\partial T + \frac{\partial\sigma}{\partial E}\partial E + \frac{\partial\sigma}{\partial C}\partial C \quad (4)$$

Where, T, E, C, σ are temperature, electric field, concentration of the solute and surface tension respectively. In pure diffusion case we are only concerned with the change in surface tension due to temperature. The dependency of the surface tension on the temperature can be expressed by Eotvos equation: [3]

$$\sigma = 0.07275 \times (1 - (0.002 \times (T - 291))) \quad (5)$$

The above equation shows that the surface tension decreases linearly with the increase in temperature. As the temperature increases the attraction or the binding force between the molecules decreases which in turn reduces the surface tension. The surface tension values for the range of temperature from 273K – 304K is shown in the plot.

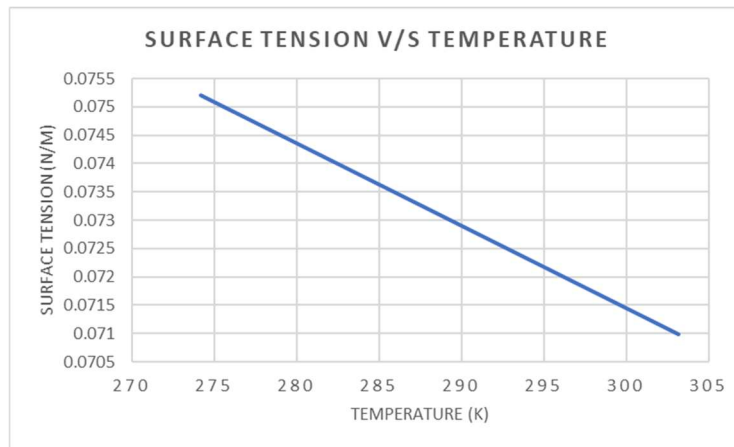


Figure 1.2 Plot of surface tension v/s temperature

Following figure explains the Marangoni convection caused due to surface tension gradient at the interface which depends on the temperature. [4]

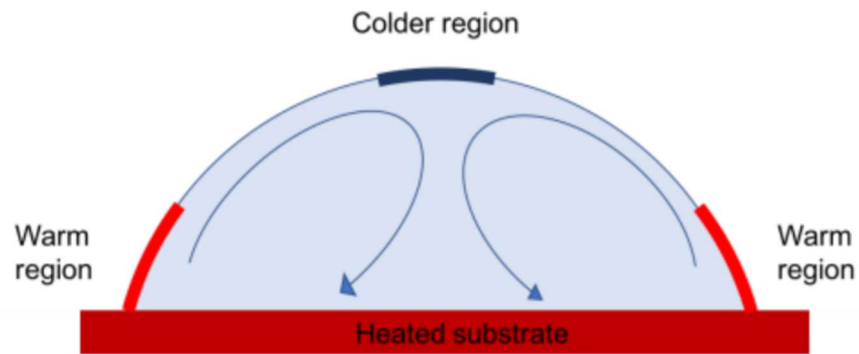


Figure 1.3 Marangoni convection in sessile droplet

As the sessile drop is resting on the heated surface the bulk liquid in the lower region will have higher temperature as compared to that of the liquid-gas interface which continuously loses mass taking away the latent heat of vaporization which reduces the temperature at the interface. Due to the inverse proportionality relation of the surface tension on temperature a gradient will be formed. The warmer region will be the region of low surface tension and the colder region will be the region of high surface tension, this imbalance creates a shear stress at the interface which results in fluid motion along the interface. Hence, the lower surface tension region will pull the fluid from the higher surface tension region along the interface which creates symmetrical vortices giving rise to Marangoni convection. This phenomenon is strongest at the interface and is also termed as thermo-capillary convection.

The internal fluid flow is caused by Marangoni convection and due to the gravity or buoyancy effects. The dimensionless number which determines the influence of both the effects is the Bond number. It is the ratio of the Rayleigh number which determines

the gravity effects to that of the Marangoni number which determines the strength of Marangoni convection.

$$Bo = \frac{\alpha \rho g H^2}{\sigma_T} \quad (6)$$

α , ρ , g , H , σ_T are the coefficient of thermal expansion, density, gravity, the height of the droplet and temperature derivative of surface tension respectively. If the $Bo < 1$, then gravity or buoyancy effects can be neglected. [5]

1.4 Governing Equations

The phenomenon taking place in the evaporation process can be expressed by different governing equations which can imitate the same process. The transport equation is responsible for the computation of mass flux at each time instant.

$$\frac{\partial c}{\partial t} + (u \cdot \nabla)c = \nabla \cdot (D \nabla c) \quad (7)$$

To obtain the solution for the flow field inside the water droplet and that of ambient air, incompressible Navier-Stokes equation is solved along with the continuity equation. Momentum conservation is represented by Navier-Stokes equation while the conservation of mass is represented by continuity equation. The solution of both these equations yields the velocity and pressure field.

$$\rho \left(\frac{\partial u}{\partial t} + (u \cdot \nabla)u \right) = \nabla \cdot [-p \cdot I + \mu (\nabla u + \nabla u^T)] + F \quad (8)$$

$$\nabla \cdot (\rho u) = 0 \quad (9)$$

To obtain the temperature field inside the droplet and ambient air the energy equation is used.

$$\rho c_p \left(\frac{\partial T}{\partial t} + (u \cdot \nabla)T \right) = \nabla \cdot (k \nabla T) \quad (10)$$

The velocity field which is obtained due to mass flux affects the temperature, thus a coupled system is solved using non-linear solver in COMSOL Multiphysics.

Chapter 2

INTERFACE TRACKING METHOD

2.1 Introduction

During evaporation the mass loss takes place across the liquid-gas interface decreasing the volume of the droplet, which results in the continuous evolution of the interface. In a numerical model to simulate such condition we need to have a method by which we can track the interface precisely which can show us the position of the interface after each time interval during which the evaporation takes place. There are many methods to do this but the one we are focusing on is the Level-set (LS) method and the Arbitrary Lagrangian Eulerian moving mesh method (ALE). Let us look at the formulation of both these methods in detail.

2.2 Level-set method (LS)

The Level-set method was first introduced in 1988 by Osher and Sethian. It is the versatile method for computing and analyzing the motion of interface in 2D and 3D. The Level-set function is constricted to the domain. The zero level set $\phi = 0$ corresponds to the evolving front.

$\phi = \phi(r,t)$, $r \in \Omega$ where, Ω is our domain of interest. The equation corresponding to the evolution of ϕ is given by a convection equation where u represents the velocity field.

$$\frac{\partial \phi}{\partial t} + u \cdot \nabla \phi = 0 \quad (11)$$

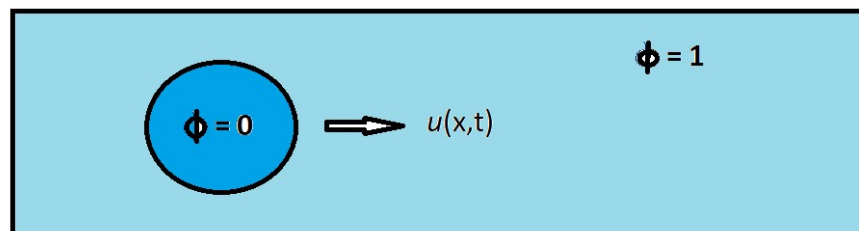


Figure 2.1 Evolving front in Level-set method.

The zero level set always gives the location of the interface. The domains on either side of the interface are distinguished by having positive value on one side and negative on the other side. Heaviside function is used to represent the density and viscosity.

$$H(\phi) = 0, \phi < 0 \quad \& \quad H(\phi) = 1, \phi > 0 \quad (12)$$

In numerical simulations to avoid an abrupt jump in the density and viscosity which causes the instability instead of using the direct delta or Heaviside function it uses smeared out Heaviside function. The density and viscosity using the smeared function is given by,

$$\begin{aligned} \rho &= \rho_1 + (\rho_2 - \rho_1)H(\phi) \\ \vartheta &= \vartheta_1 + (\vartheta_2 - \vartheta_1)H(\phi) \end{aligned} \quad (13)$$

As compared to the physical situation in which the interface is not separated by a distinct boundary, but to track it in the numerical domain we must have a certain thickness of the interface in the numerical domain. Now, to track and maintain the constant thickness of the interface an intermediate step is performed by adding an artificial flux and to avoid the discontinuities at the interface a viscosity term is added. The modified equation will look like,

$$\frac{\partial \phi}{\partial t} + \nabla \cdot (u\phi) = \epsilon \nabla^2 \phi - \nabla \cdot f(\phi) \quad (14)$$

$$f = \phi(1 - \phi) \frac{\nabla \phi}{|\nabla \phi|} \quad (15)$$

Where, $f(\phi)$ is the artificial flux. ϵ is the interface thickness. The Laplacian term on the right-hand side can be termed as the diffusive term that enlarges with the width of the interface during the simulation, to counteract this we have the divergence of the artificial flux subtracted from it. When the interface thickness is equal to ϵ both the terms on the right-hand side will be in equilibrium and will become zero. Thus, the constant interface thickness is achieved. [6,7]

COMSOL Multiphysics uses the equation (14) to track the evolving interface and this equation is always coupled to the laminar flow physics because it uses the velocity field computed by Navier-Stokes equation.

2.3 Arbitrary Lagrangian Eulerian moving mesh (ALE)

There are two ways in which the partial differential equations of physics are formulated in the coordinate system. The basic difference lies in the description of the properties specified at the nodes, if the axes of the coordinate system are fixed in space then the properties will only change with time such coordinate system is called the spatial coordinate system and the formulation is a Eulerian formulation. If the coordinate system is fixed to the material and the nodes deform with the material, then the properties now will become the function of space and time such coordinate system is called the material coordinate system and the formulation is Lagrangian formulation.

If we want to simulate the properties at specified points fixed in space involving gases and liquids it is not possible to track the individual particles, thus in such cases Lagrangian description is not feasible. On the other hand, the Eulerian formulation cannot handle the moving boundary problem as the quantities are referred to fixed points in space. Now, to simulate the evaporation of the droplet and track the evolving interface during the evaporation we need the qualities of both the coordinate system. Thus, to overcome the drawbacks of both the spatial and material coordinate system this method introduces a third coordinate system called the mesh coordinate system.

If we coincide the mesh frame with the material frame of reference so that it may deform with the material, now if can map this deform coordinates on the fixed spatial frame then we can take the advantage of both the formulation techniques. So is the name

Arbitrary Lagrangian Eulerian moving mesh (ALE). The following example shows how the ale mesh works. [8,9]

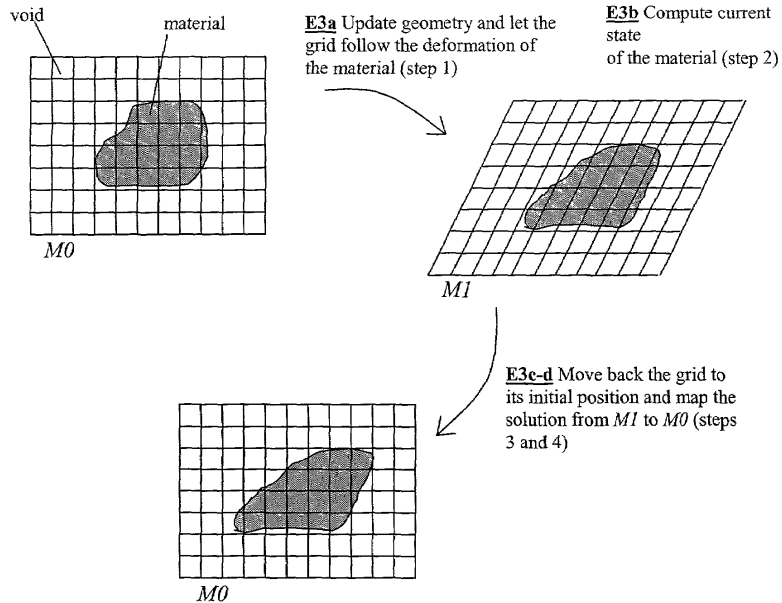


FIG. 6

Figure 2.2 ALE moving mesh method.

As shown in the figure all the frames spatial, material and mesh are identical at first, now as the simulation starts the mesh frame gets deformed with the material frame which is shown by the frame M1. The deformed nodes now get mapped to the spatial coordinates and we can see the deformation in the material compared to the initial stage which is shown in the frame M0. The quality of mesh gets deteriorated with time due to the mapping from mesh to spatial coordinates. To eliminate such issue remeshing operation can be done by stopping the simulation and creating the new mesh in the present configuration and mapping all the properties to the new mesh. The simulation will start from where it had stopped as all the properties have been identified internally and

mapped to the spatial coordinates. Thus, ALE is intermediate and combines the advantages of both the formulations. Now we will study the formulation of PDE in the ALE frame. [8]

Let the material coordinates and mesh coordinates be denoted by X and X_m respectively. The spatial coordinates of the specified material/mesh nodes are expressed as $x(X,t)$ and $x(X_m,t)$ at time t respectively. The material derivative will be different in different frames and can be obtained by applying the chain rule.

In the Lagrangian frame, the material nodes are constant. Hence,

$$\begin{aligned}\frac{Dx}{Dt} &= \left. \frac{\partial x}{\partial t} \right|_X + \frac{\partial X}{\partial X} \cdot \left. \frac{\partial x}{\partial t} \right|_X \\ &= \left. \frac{\partial x}{\partial t} \right|_X + 0 = u(X, t) \text{ which is the velocity of material.}\end{aligned}\quad (16)$$

In Eulerian frame, material derivative for ant field function f is given by,

$$\frac{Df}{Dt} = \left. \frac{\partial f}{\partial t} \right|_x + \frac{\partial f}{\partial x} \times \left. \frac{\partial x}{\partial t} \right|_X \quad (17)$$

If the field function f is replaced by the spatial coordinate x then we get,

$$\begin{aligned}\frac{Dx}{Dt} &= \left. \frac{\partial x}{\partial t} \right|_x + \frac{\partial x}{\partial x} \times \left. \frac{\partial x}{\partial t} \right|_X \\ &= \left. \frac{\partial x}{\partial t} \right|_x + u(X, t)\end{aligned}\quad (18)$$

In ALE frame,

$$\begin{aligned}\frac{Dx}{Dt} &= \left. \frac{\partial x}{\partial t} \right|_{X_m} + \frac{\partial x}{\partial X_m} \times \left. \frac{\partial X_m}{\partial t} \right|_X \\ &= u(X_m, t) + \frac{\partial x}{\partial X_m} \times \left. \frac{\partial X_m}{\partial t} \right|_X\end{aligned}\quad (19)$$

If we combine the equation (16) and (19) we get,

$$\left. \frac{\partial x}{\partial X_m} \times \frac{\partial X_m}{\partial t} \right|_X = u(X, t) - u(X_m, t) \quad (20)$$

Where, $\left. \frac{\partial x}{\partial X_m} \times \frac{\partial X_m}{\partial t} \right|_X$ is called the convective velocity given by, u_c .

Now if we express material derivative of a field function f in ALE frame, it is given as:

$$\left. \frac{Df}{Dt} = \frac{\partial f}{\partial t} \right|_{X_m} + \left. \frac{\partial f}{\partial x} \times \left(\frac{\partial x}{\partial X_m} \times \frac{\partial X_m}{\partial t} \right) \right|_X \quad (21)$$

Substitute equation (20) into (21) we get,

$$\left. \frac{Df}{Dt} = \frac{\partial f}{\partial t} \right|_{X_m} + (u_c \cdot \nabla) f \quad (22)$$

If we compare the equation (22) with that of the material derivative in the Eulerian frame for any field function f i.e. equation (17) we will notice that $u(X,t)$ is replaced by u_c . Thus, the modified governing equation in the ALE frame will be as follows: [6]

- Navier-Stokes equation:

$$\rho \left(\frac{\partial u}{\partial t} + (u_c \cdot \nabla) u \right) = \nabla \cdot [-p \cdot I + \mu (\nabla u + \nabla u^T)] + F \quad (23)$$

- The transport-diffusion equation:

$$\frac{\partial c}{\partial t} + (u_c \cdot \nabla) c = \nabla \cdot (D \nabla c) \quad (24)$$

- The energy equation:

$$\rho c_p \left(\frac{\partial T}{\partial t} + (u_c \cdot \nabla) T \right) = \nabla \cdot (k \nabla T) \quad (25)$$

Here, the convective velocity has been introduced as an additional degree of freedom which can be controlled by specifying the mesh velocity. Winslow smoothing method is used in COMSOL Multiphysics for smoothly deforming the mesh and regenerate the interior mesh nodes according to the prescribed boundary condition.

Chapter 3

NUMERICAL STUDY

3.1 Introduction

COMSOL Multiphysics is a commercially available software to do the numerical simulation. It is basically a finite element analysis software which discretizes the partial differential equations by using the finite difference method and solves this discretized equation at each mesh nodes to obtain the solution. The PDE's such as the Navier-Stokes or energy equation cannot be solved manually for complex coupled problem along with other equations prescribed with boundary conditions such as the present model. Hence, in such situations the software becomes handy wherein it approximates the numerical model of PDE's and solves it by using various numerical models.

3.2 Modelling

A two-phase 2D model was built in COMSOL. Pure diffusion model was studied to track the interface using the Level-set and ALE moving mesh method. Due to the drawbacks of the Level-set method, the ALE moving mesh method was adopted to study the influence of Marangoni convection on evaporation in pure diffusion model using two cases one in which Marangoni convection was not considered and the other case considering the same. Modelling has four steps. The first involves the building of geometry which imitates the real system as much as possible, second is to select the physics pertaining to the situation and its coupling with the involved physics, the next step is meshing in which the model is breakdown into numerous fine elements which is followed by obtaining the solution for the PDE's of each discretized element.

3.3 Assumptions

Following assumptions were made for the numerical model:

1. The droplet is the spherical cap having a 90° contact angle.
2. The droplet is assumed to be pinned during evaporation so there will be no change in the contact area only the contact angle will decrease.
3. The flow in the fluids i.e. air and water is incompressible.
4. All the properties are constant and do not change with temperature and pressure unless it is specified.
5. No external convection of air is considered.
6. The buoyancy effects due to gravity are neglected as they are insignificant.

3.4 Pure diffusion model using Level-set method

The two-phase laminar flow with the level set, transport of diluted species and heat transfer in fluids physics are used to simulate the evaporation of droplet. Here, the transport of diluted species is separately applied for air and water domain for the ease of specifying the variable and the flux continuity is taken care of by specifying flux at the interface.

3.4.1 Transport of diluted species (Air & water)

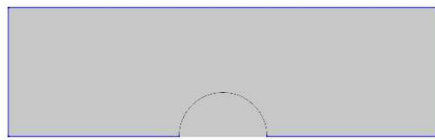
For Air domain,

- Initial conditions:

Initial concentration is given to the air domain at the ambient temperature of 293.15K. The relative humidity (H) is 20%, universal gas constant (R) is 8.314 (J/mol.K) and the saturated vapor pressure corresponding to the ambient temperature is 2333.3 kPa. The concentration is calculated by: $c = \frac{P_{v,sat} \times H}{R \times T}$.

- Boundary conditions:

The no-flux condition is given at the outer boundaries of the air domain. The flux condition is applied at the interface. The equation for flux is $M \cdot (c_2 - c)$, where M is the mass transfer coefficient specified in m/s, it plays the same role as the diffusion coefficient. c_2 is the saturated concentration at the interface and c is concentration of ambient air. The figure shows the BC's applied on the domain.



No flux $\mathbf{n} \cdot \nabla c = 0$



Flux at interface $M \cdot (c_2 - c)$

Figure 3.1 BC for transport of diluted species in air domain.

For water domain,

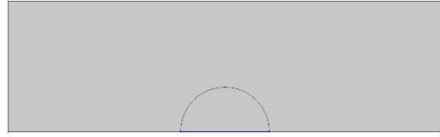
- Initial conditions:

Saturated concentration at the ambient temperature is given as initial condition to

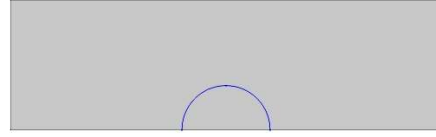
water domain. The equation for the saturated concentration is given by $c_2 = \frac{P_{v,sat}}{R \times T}$.

- Boundary condition:

The no-flux condition is given at the bottom of the water domain and the flux condition at the interface is given by $-M \cdot (c_2 - c)$. As the water domain losses mass so the flux is negative and vice versa case for air domain. Hence, flux continuity is maintained.



No flux $\mathbf{n} \cdot \nabla c = 0$



Flux at interface $-M \cdot (c_2 - c)$

Figure 3.2 B.C for transport of diluted species for water domain.

3.4.2 Laminar flow

- Initial conditions:

The initial fluid velocity and pressure for both air and water domain is specified as 0 m/s and 0 Pa respectively. The boundaries of water domain are selected as an Initial interface.

- Boundary condition:

No slip condition i.e. $u=0$ is specified at outer boundaries of both the domain.

The mass balance at the interface is given by a weak contribution condition in COMSOL Multiphysics. The equation for mass balance is as follows: [10]

$$(p_g - p_l)I + \mu_l(\nabla u + (\nabla u)^T)_l - \mu_g(\nabla u + (\nabla u)^T)_g = (\sigma\kappa - v_{lg} \dot{m}^2) \quad (26)$$

Here the Navier-Stokes equation is balanced by the right-hand side term where σ , κ are surface tension and curvature respectively. \dot{m} is the mass flux and v_{lg} is the inverse difference of densities of both the fluids given by $v_{lg} = \rho_g^{-1} - \rho_l^{-1}$.

3.4.3 Heat transfer in fluids

- Initial conditions:

The initial temperature of both the domains is kept at the ambient temperature

which is 293.15 K.

- Boundary condition:

The outer boundaries of both the domains are insulated i.e. $-n \cdot q = 0$. The interface acts as the boundary heat source for the water domain because it loses the latent heat of vaporization. The boundary condition prescribed at the interface is $-H_{vap} \times c_{2_lm}$ where, H_{vap} is the latent heat of vaporization, 40641 (J/mol) and c_{2_lm} is the Lagrange multiplier which predefined in the COMSOL library. [11]

3.4.4 Multiphysics coupling

Heat transfer in fluids is coupled with the transport of diluted species as the vapor pressure is the function of temperature through which the concentration is calculated. An interpolated function is developed in COMSOL Multiphysics which interpolates the value corresponding to the calculated temperature by the energy equation and the concentration at the interface is evaluated.

The below figure gives an insight how the calculation proceeds:

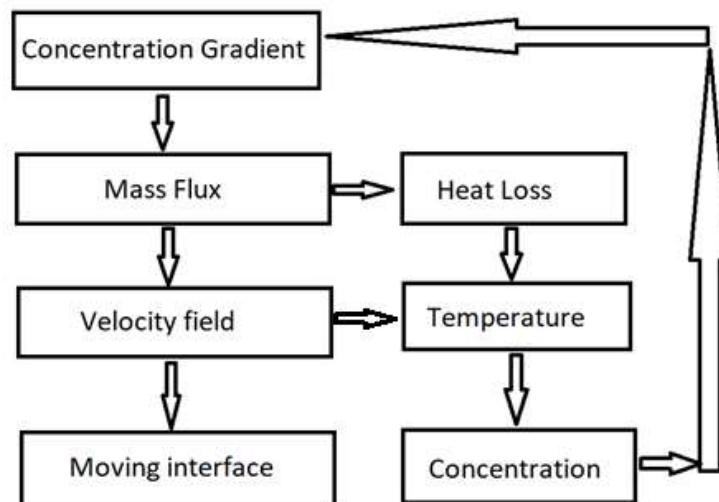


Figure 3.3 Physics coupling and calculation steps.

The concentration gradient will be produced due to the difference in the saturated concentration at the interface and the ambient air, this will lead to the mass flux from the water domain to the air which is evaluated from transport-diffusion equation. As the water vapor enters the ambient air there will be variation in the pressure and velocity fields which will be taken care of by Navier-Stokes equation, in turn this velocity field will be used by the Level-set equation to track the interface.

The heat of vaporization is lost due to the outgoing mass flux at the interface which reduces the temperature. Hence, the temperature of the bulk water is reduced with the time. The concentration at the interface is again calculated corresponding to this temperature and the cycle continues. The velocity field influences the temperature in both the fluids, so the arrow is shown in the figure.

3.4.5 Results

1. The volume fraction of the fluid with the time.

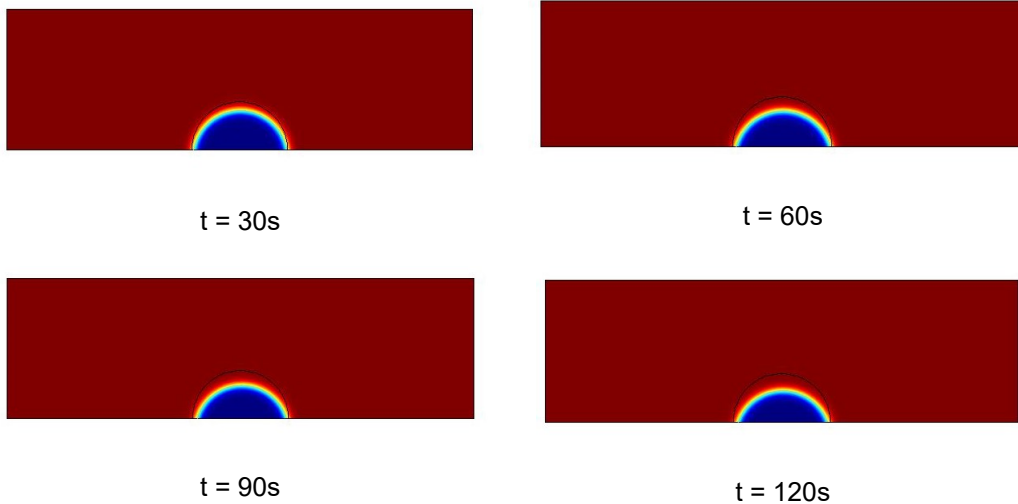


Figure 3.4 Volume fraction of fluid with time.

2. The concentration at the interface with time.

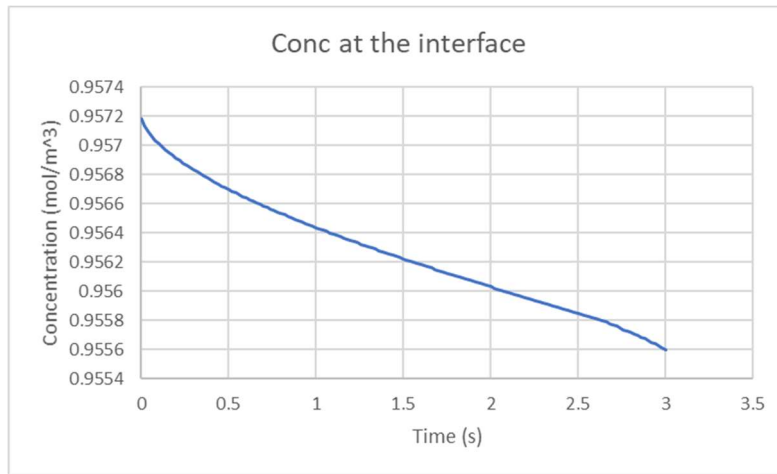


Figure 3.5 Concentration at the interface with time.

The figure shows that concentration at the interface decreases continuously with the time. As the heat of vaporization is lost due to the mass flux coming out from the interface, so the vapor pressure decreases with the time as it is a function of temperature and as a result concentration also decreases.

3. Temperature of the bulk water.

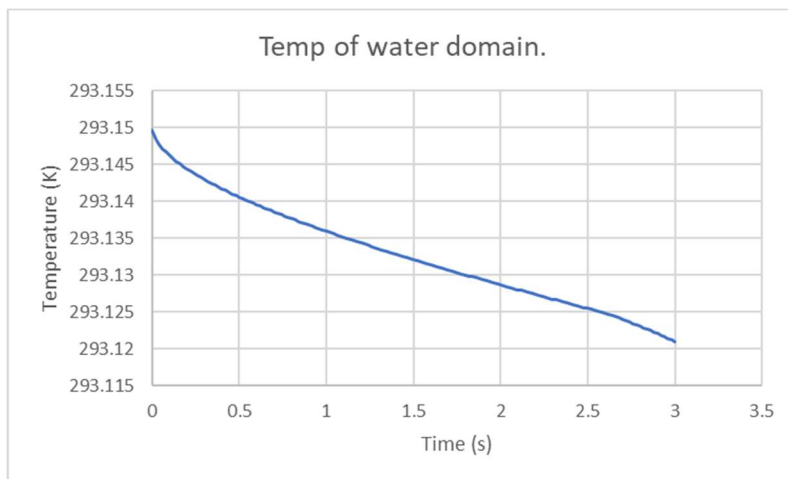


Figure 3.6 Average temperature of the bulk liquid.

3.4.6 Conclusion

- 1) The mass conservation is not satisfied when the non-conservative Level-set equation is used. So, we encounter the abrupt mass loss from a droplet in just 2s.
- 2) The change in concentration at the interface cannot be validated. The boundary condition of saturated concentration is given on initial interface, so we do not know whether the condition moves with the boundary or not.
- 3) The position of the interface cannot be validated to be exactly as the same amount as that of the mass loss taking place from the interface.
- 4) The Level-set equation used in COMSOL Multiphysics is the Cahn-Hillard equation which uses the velocity field for tracking the interface.
- 5) This equation in COMSOL Multiphysics cannot handle the phase change problem, because the boundary condition on the interface cannot be made a function of Level-set parameter ϕ as it overwrites the value of $\phi = 1$ assigned for the water domain.

Level-set can only be used in situations when there is an interaction between two distinct fluids and due to that interaction, there will be a change in the position of the interface which is influenced by the velocity field in both the fluids. e.g. oil in water.

3.5 Pure diffusion model using ALE moving mesh without Marangoni convection

The laminar two-phase flow with ale moving mesh module is used along with the transport of diluted species and heat transfer in fluids. The numerical model has the curved edges so that the meshing is smooth and it does not get deteriorated during remeshing.

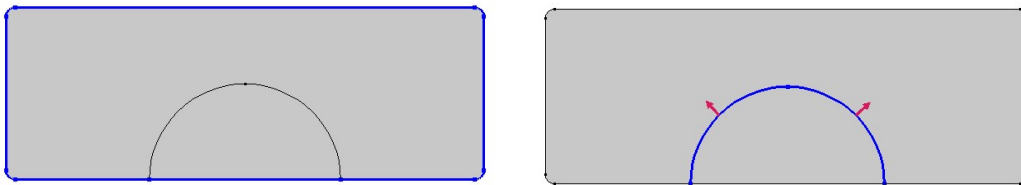
3.5.1 Laminar two-phase flow with moving mesh

- Initial conditions:

The initial velocity, pressure and temperature for the whole domain are specified to be 0 m/s, 0 Pa and 293.15 K respectively. The initial condition for the mesh displacement in both the domains is given as 0 for both X & Y directions.

- Boundary condition:

The surface tension at the interface is given a constant value of $7.2e-2$ N/m as we are not considering the effect of Marangoni convection. At the fluid-fluid interface mass flux condition is prescribed acting in the normal direction as shown in the figure.



No slip, $u = 0$

Mass flux = $-mf$, $\sigma = 7.2e-2$ N/m

Figure 3.7 B.C for laminar flow

The mesh velocity is calculated from the mass flux condition provided at the fluid-fluid interface. The mass flux is calculated from the transport of diluted species and by the continuity & Navier-Stokes equation it gets converted into the interface or mesh velocity.

$$-mf = tds.ntflux_c \times M_w \quad (27)$$

where, $tds.ntflux_c$ is the predefined normal mass flux and M_w is the molecular weight of water which is 18.015 g/mol.

The mass balance at the interface:

$$u_l \rho_l n = u_g \rho_g = -mf \cdot n$$

$$u_g - u_l = (\rho_g^{-1} - \rho_l^{-1}) \cdot (-mf) \cdot n \quad (28)$$

COMSOL Multiphysics uses SIMPLE (Semi-Implicit method for pressure linked equation) algorithm to solve the Navier-Stokes and continuity equation. The velocity is calculated from Navier-Stokes equation and is checked for the conservation of mass in the continuity equation. Thus, it reciprocates between both the equations until the mass balance equation (28) is satisfied; from this we obtain the velocity of both the water and the air domain. This velocity is taken as the input to calculate the mesh velocity as shown below: [12]

$$u_{mesh} = \left(u_l \cdot n + \frac{mf}{\rho_l} \right) \cdot n \quad (29)$$

3.5.2 Transport of diluted species

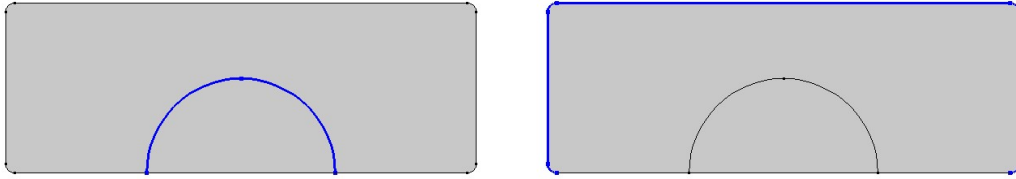
Only air domain is selected for this physics.

- Initial conditions:

The ambient air concentration which is 0.1912 (mol/m³) is given in the air domain.

- Boundary conditions:

The interface is given the saturated concentration which is temperature dependent and the outer boundaries of the gas domain are given the ambient concentration. The bottom boundaries are given the no-flux condition which is $n \cdot \nabla c = 0$. The diffusion coefficient is defined as $D = 2.82e-5$ (m²/s).



$$\text{Concentration } (c_2) = \frac{P_{v,sat}(T)}{R \times T}$$

$$\text{Concentration } (c_1) = 0.1912 \text{ (mol/m}^3\text{)}$$

Figure 3.8 B.C. for transport of diluted species.

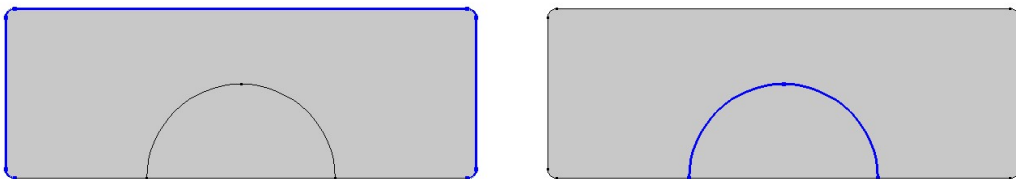
3.5.3 Heat transfer in fluids

- Initial conditions:

The air and water domain both are the ambient temperature of 293.15 K.

- Boundary conditions:

The outer boundaries of the gas domain are at the ambient temperature. The interface acts as the boundary heat source because it is responsible for the loss of heat from the water domain due to the mass flux coming out across it. The bottom boundaries are insulated given by $-n \cdot q = 0$.



$$T_0 = 293.15 \text{ K}$$

$$\text{Boundary heat source, } Q_b = -H_{\text{vap}} * c_{2_l} m$$

Figure 3.9 B.C. for heat transfer in fluids.

3.5.4 Meshing

A non-uniform meshing was done to precisely track the movement of the Interface. Free triangular elements whose size were in the range of 0.03mm to 0.005mm were used. The elements were densely populated near the interface and the bottom boundaries as shown.

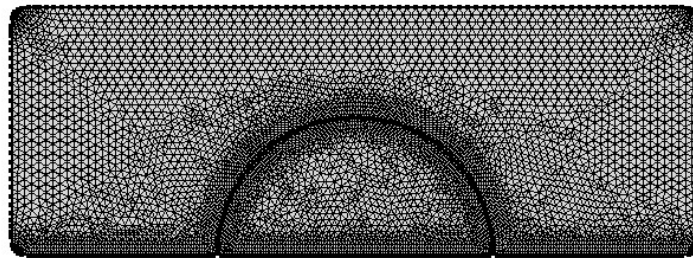
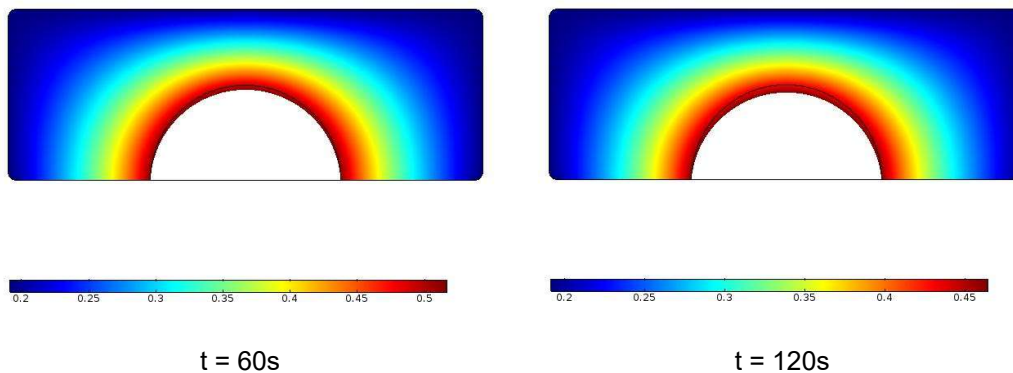


Figure 3.10 2D Meshing using free triangular elements.

3.5.5 Results

1. Concentration at the interface.



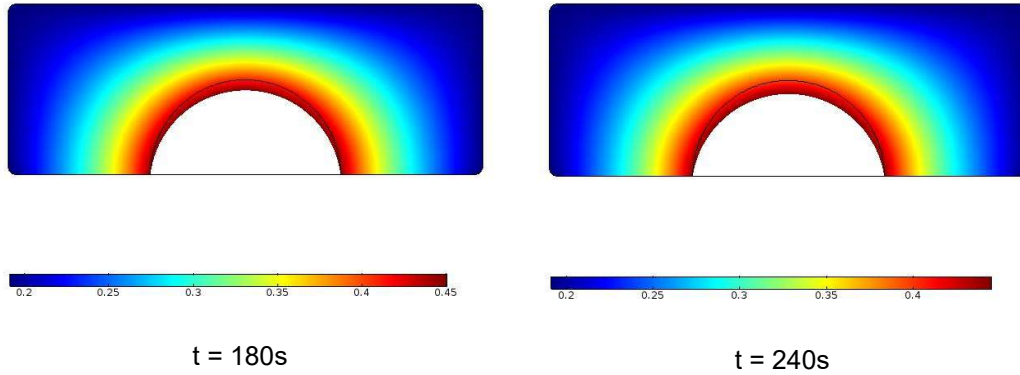


Figure 3.11 Concentration across the interface with time.

The plot for the concentration is as below:

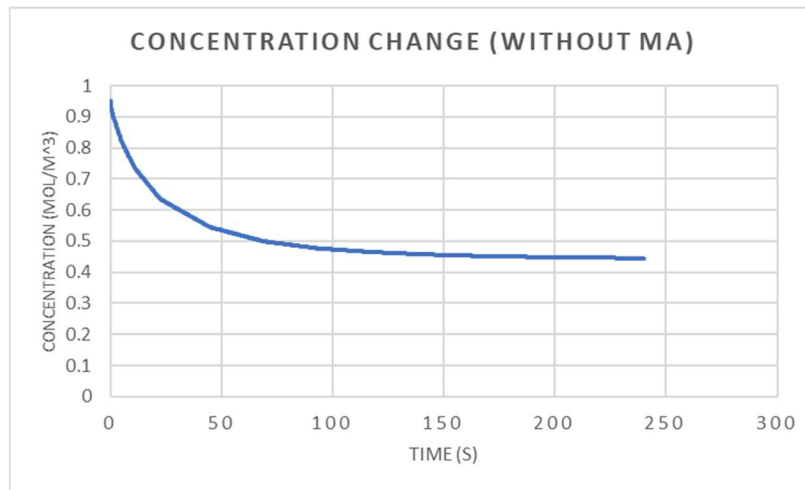


Figure 3.12 Plot for the concentration (without MA).

The vapor pressure decreases with the temperature so the saturated concentration at the interface decreases with time. As, the gradient between the interface concentration and that of air decreases with the time we can see that it becomes almost constant after 100s.

2. Average temperature of the water droplet.

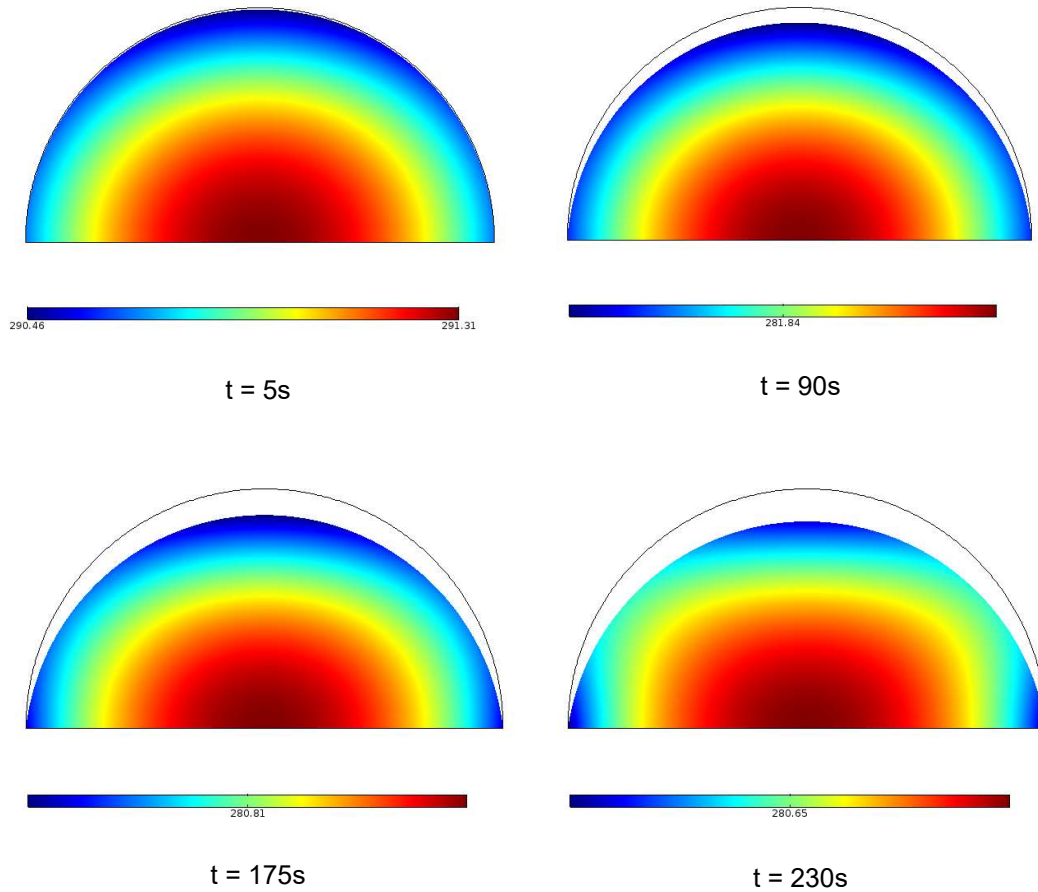


Figure 3.13 Average temperature of the water droplet.

The temperature profile here is symmetric, here the interface loses the heat, so the temperature is less as compared to that of the bulk liquid. The plot shows that the temperature decreases rapidly during the range of 0-100s, this is due to the mass flux going out because of the concentration gradient which decreases eventually as shown in the plot below.

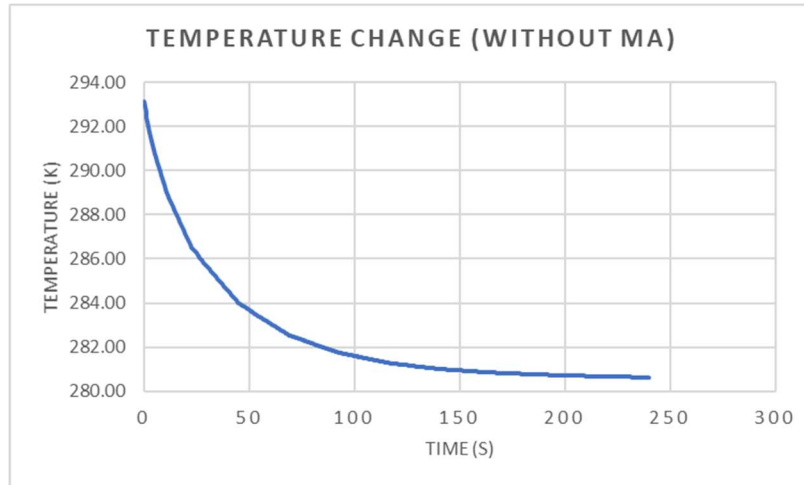


Figure 3.14 Temperature of the water droplet (without MA).

3.6 Pure diffusion model using ALE moving mesh with Marangoni convection

All the assumptions and the boundary conditions as shown in the previous model are same in the present model except the surface tension, which now has become a function of the temperature and is specified at the interface. The tangential component of the shear stress at the interface must balance the tangential stress arising from the gradient in surface tension which is given by the equation: [13,14]

$$\nabla \cdot [-p.I + \mu (\nabla u + \nabla u^T)] = \sigma \nabla_t T \quad (30)$$

3.6.1 Results

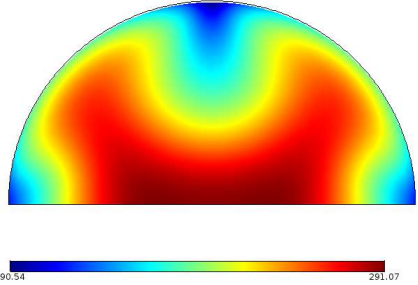
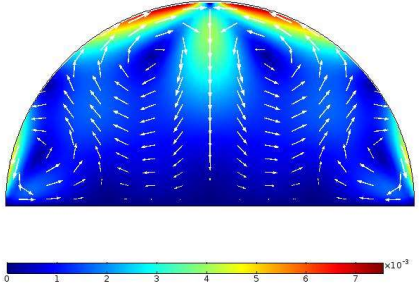
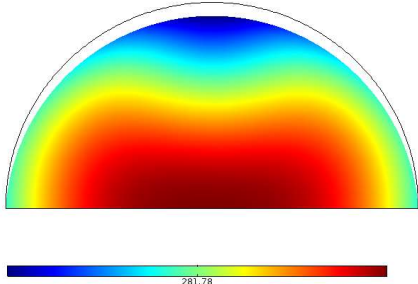
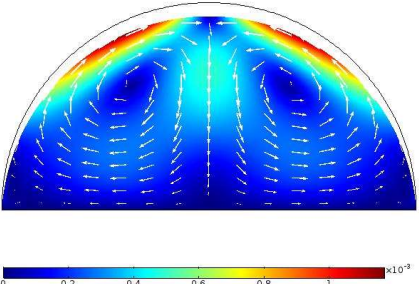
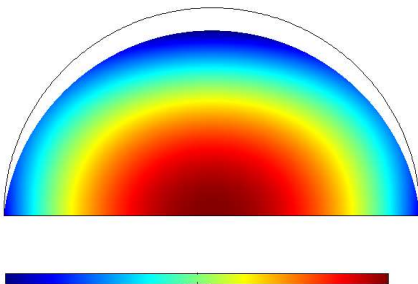
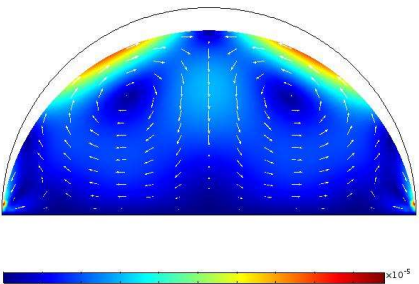
1. Concentration at the interface.

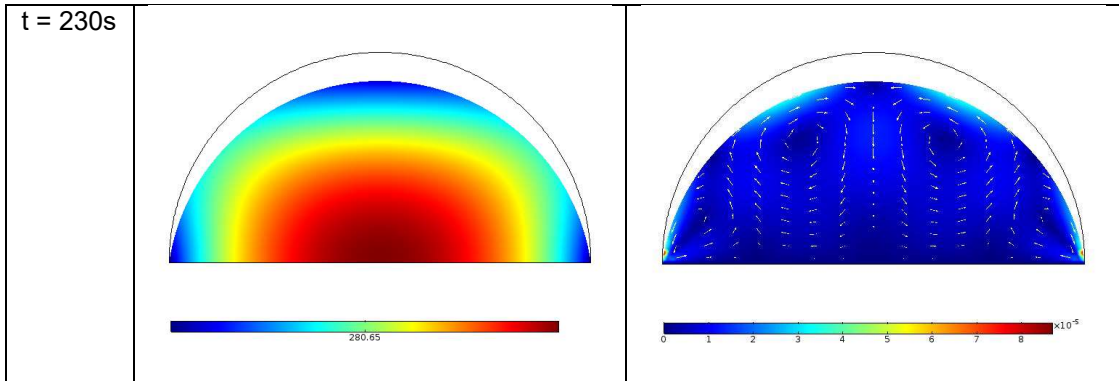
The same trend is followed in the simulation for the concentration at the interface, there is negligible change in the value noticed after the second decimal point in comparison to the previous model.

2. Temperature and velocity field of the water droplet.

The table shows the velocity profile corresponding to the temperature profile.

Table 1 Velocity and temperature profile of droplet (with MA).

Time	Temperature Profile	Velocity Profile
t = 5s		
t = 90s		
t = 175s		



We can clearly see the difference in the temperature profile in the range of 0-90s in which the heat is being distributed in the bulk liquid due to the Marangoni convection as compared to the previous model. Even though the temperature profile seems to be similar to the previous model in the remaining time frame, this is because the Marangoni convection is still there, but the velocity is too low which is depicted in the corresponding velocity map.

3.7 Comparison of pure diffusion model with and without Marangoni convection

1. Average temperature of the water droplet.

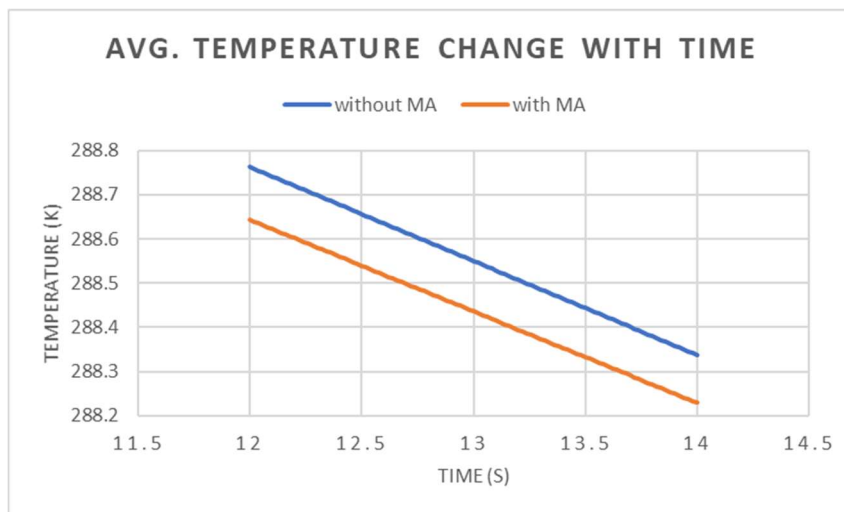


Figure 3.15 Plot of average temperature with and without MA.

The average temperature of the droplet is lower in the case when Marangoni effect is considered i.e. the evaporation rate is more. This is because the heat is distributed by the Marangoni convection inside the bulk liquid which maintains the temperature at the interface as compared to the case in which Marangoni is not considered which is shown in the figure 3.16. As the temperature is maintained at the interface the concentration corresponding to that temperature will be high as compared to the case in which Marangoni is not considered, so the concentration gradient will persist for a longer time and more mass flux will be carried out from the interface which is shown in the figure 3.17.

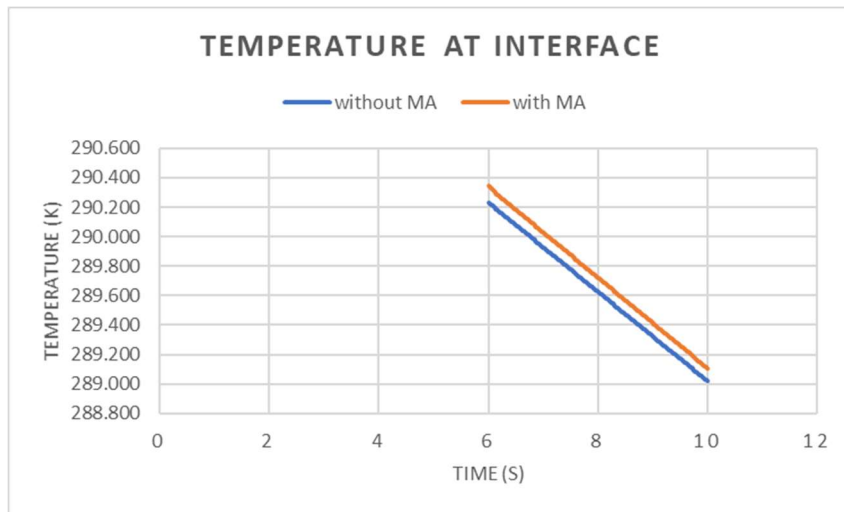


Figure 3.16 Temperature at the interface with and without MA.

The mass flux is multiplied with the molecular weight of water and the surface area of the droplet to obtain the evaporation rate in (kg/s).

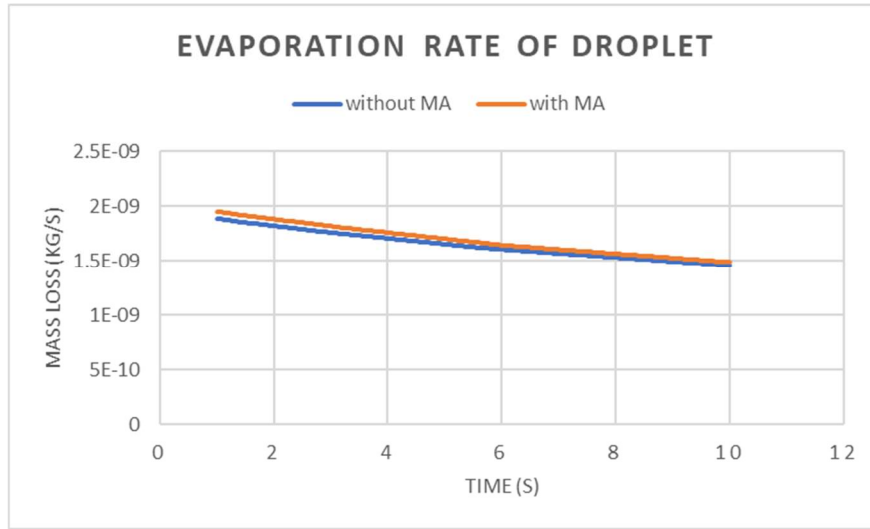
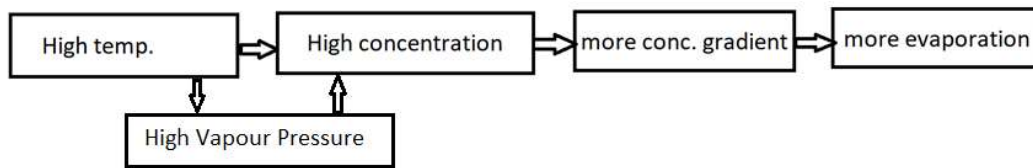


Figure 3.17 Evaporation rate of droplet with and without MA.

3.7.1 Summary

1. Evaporation rate is higher when Marangoni convection is considered.
2. Average temperature drop of the droplet is more with Marangoni convection.
3. The temperature at the interface is high with Marangoni convection as compared to without Marangoni convection.



At the interface there will be high vapor pressure due to high temperature which in turn will give high concentration at the interface producing more concentration gradient thus the evaporation rate will be high.

Chapter 4

EXPERIMENTAL VALIDATION

4.1 Introduction

An experiment is conducted to see the evaporation rate of the droplet, a $7\mu\text{L}$ droplet is kept on the glass substrate in the ambient environment and left to be evaporated. The droplet is captured at every 10s interval for capturing the shrinking interface. The base and the height of the droplet is measured by using the image processing application. The droplet takes approximately 20 mins to be evaporated completely into the atmosphere. The time interval for which the simulation takes place is 4 mins (240s) so the data has been sorted out for the same time interval. The measurements taken of the droplet with the image processing application are plotted for the height of the droplet with time shown in the figure 3.18. The base diameter of the droplet remains constant for the simulation time interval which is 4.32 mm. [15]

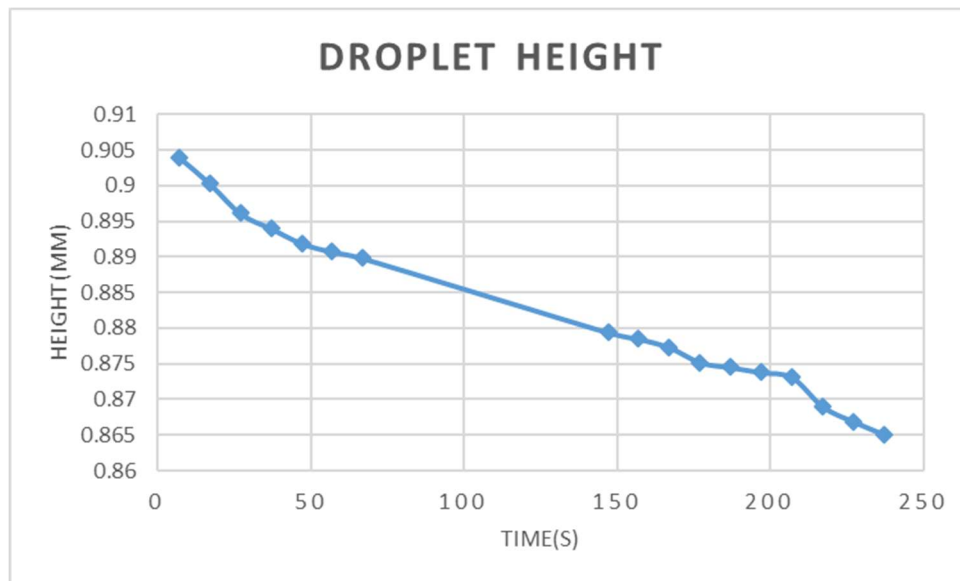
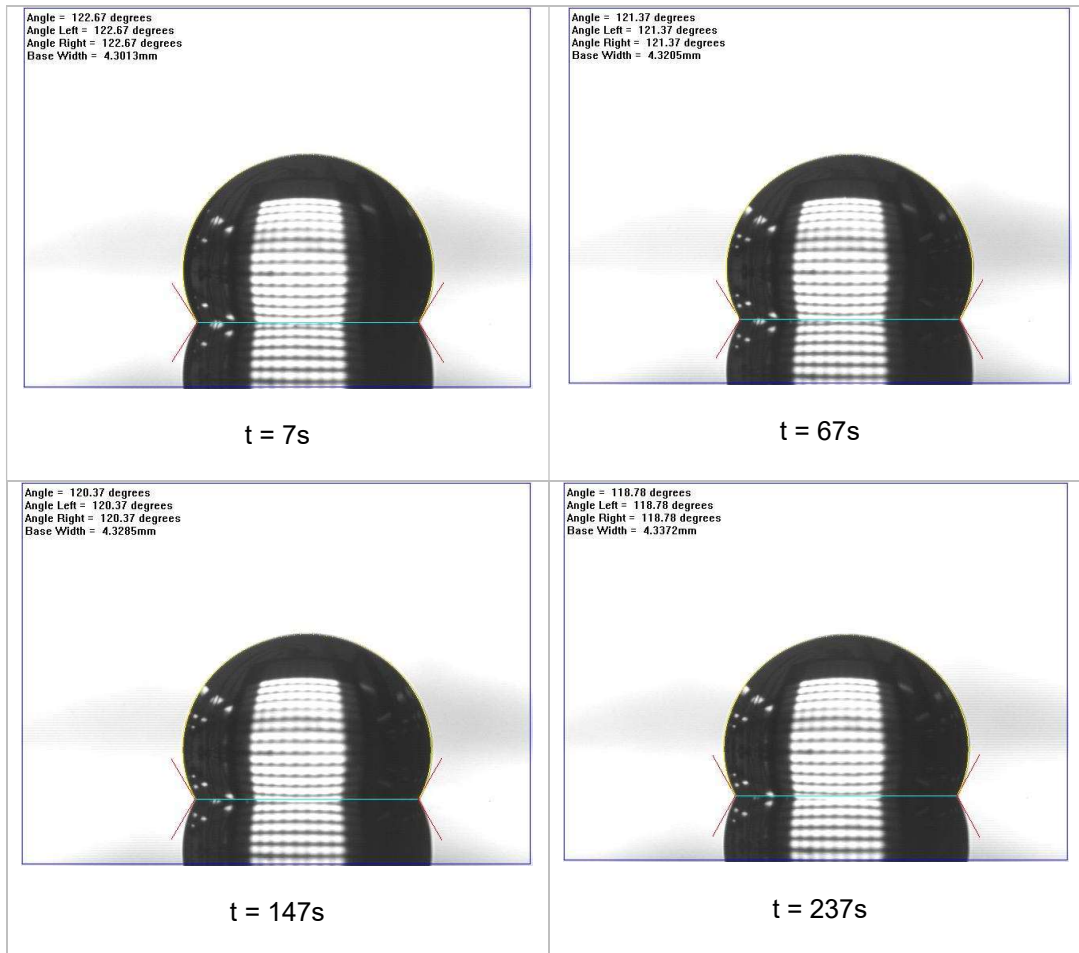


Figure 4.1 Plot of droplet height.

The following table shows the droplet at various time instances.

Table 2 Droplet evaporation at various time instances.



4.2 Image processing

- From Experiment,
 - Initial volume of droplet (V_1): $7\mu\text{L}$
 - Base diameter (c): 4.32 mm
 - Height of the droplet (h): 0.903 mm (at $t = 7\text{s}$)

0.866 mm (at t = 237s)

- Final volume of the droplet (V_2): $\frac{\pi}{6} h \left(3 \left(\frac{c^2}{4} \right) + h^2 \right)$
 $= 6.694 \mu\text{L}$
- Mass loss during 240s: $V_2 - V_1$
 $= 0.305 \mu\text{L}$

The measurements of the droplet taken with the image processing application are taken as shown in the figure below.

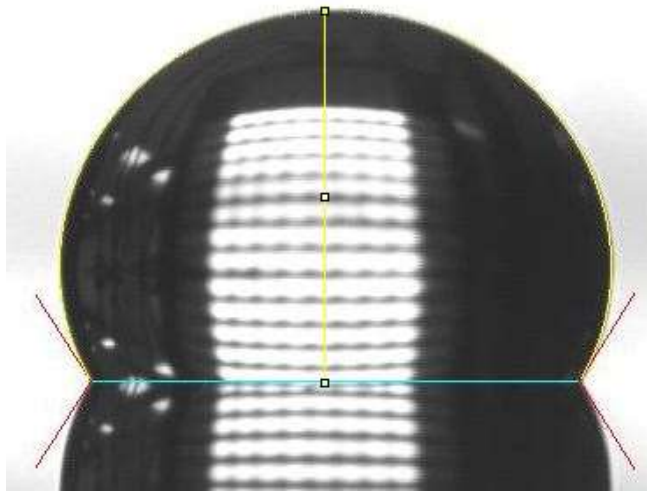


Figure 4.2 Droplet measurements taken using image processing.

- From simulation,
 - Base diameter (c): 2 mm
 - Height of the droplet (h): 1 mm (at t = 0s)
0.86 mm (at t = 240s)
 - Initial volume of the droplet (V_1): $\frac{2}{3} \pi c^2 h$
 $= 2.094 \mu\text{L}$
 - Final volume of the droplet (V_2): 1.801 μL

- Mass loss during 240s: $V_2 - V_1$
 $= 0.293\mu\text{L}$

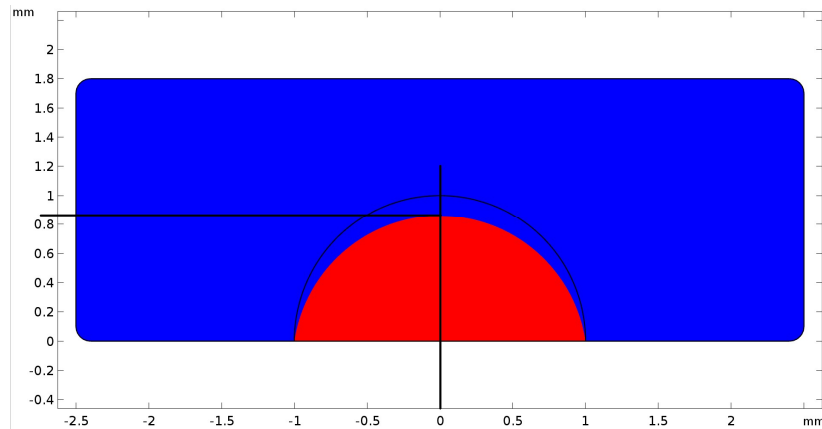


Figure 4.3 Numerical model in COMSOL Multiphysics.

The formulas for the volume of the droplets mentioned above yields the same result, the only difference is the upper one is used when the height is known and the latter one when the radius is known.

- Error estimation,
 % Mass loss (Exp.) = 4.37%
 % Mass loss (Num.) = 13.8%
 % Error = Num. value – Exp. Value
 $= 9.43\%$

The error is due to the following reasons:

- The initial volumes of the droplets are different.
- No external air convection is considered.
- The ambient relative humidity is different.
- The ambient temperature and contact angles of the droplets are different.

Chapter 5

DROPLET EVAPORATION ON HEATED SUBSTRATE

5.1 Introduction

The droplet is placed on the heated glass substrate which is maintained at 323.15K. The governing equations and the boundary conditions are same as the previous models. An additional condition of the temperature is given on the liquid-solid interface and all the other boundaries are insulated. The simulation time is reduced to 120s.

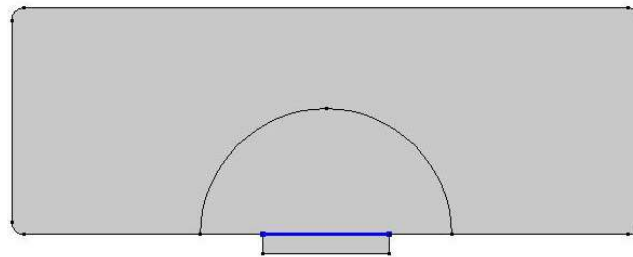
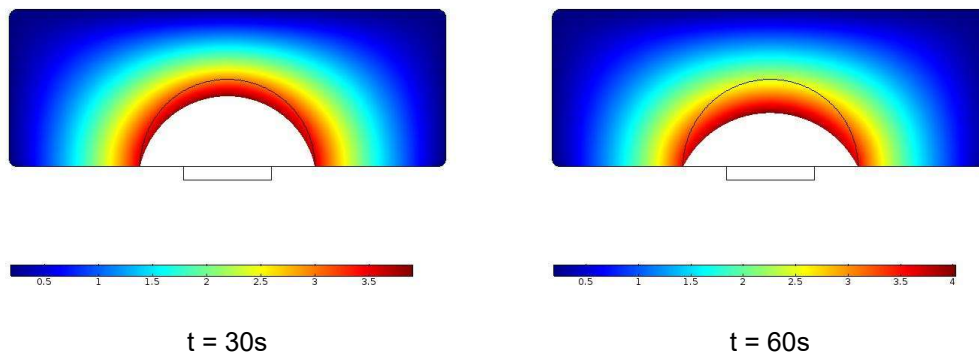


Figure 5.1 Temperature condition at the liquid-solid interface.

5.2 Results

1. Concentration at the interface.



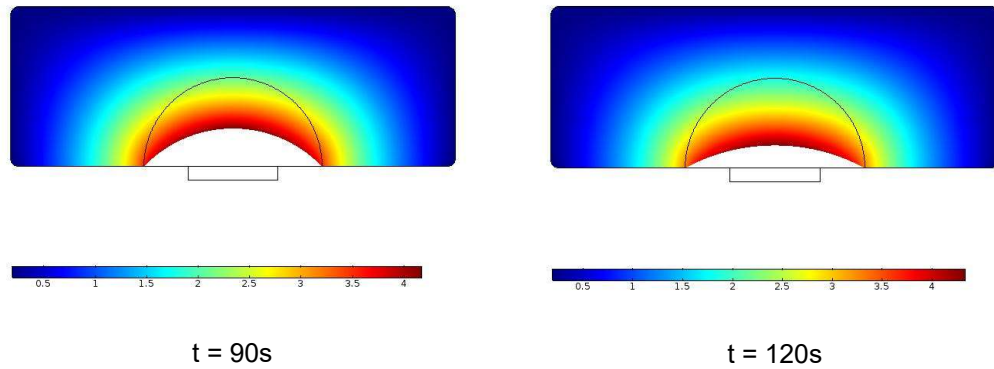


Figure 5.2 Concentration at the interface with time.

2. Average temperature of the droplet interface.

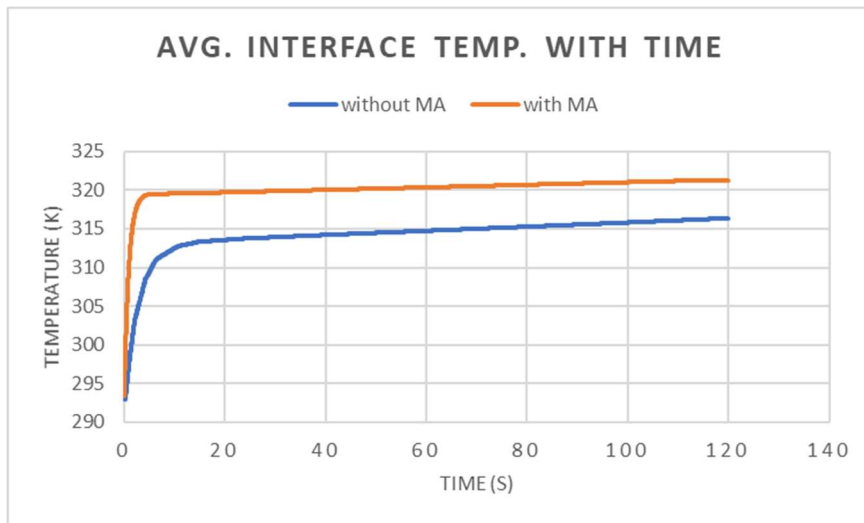


Figure 5.3 Plot of average droplet temperature with time.

We can see that the temperature increases drastically within the first 5s when the Marangoni convection is considered while it takes some time when there is no convection. After 5s we can see that the temperature increase is only $2^{\circ}C$ for the

remaining simulation time thus, concluding that the substrate is been cooled down. The clear understanding can be made by modifying the temperature boundary condition and making it the heat flux condition.

3. Average mass flux across the interface with time.

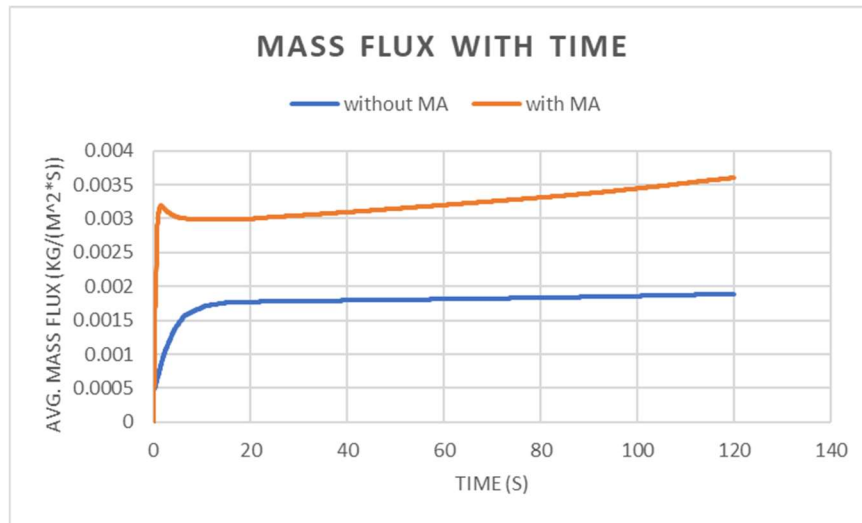


Figure 5.4 Plot of average mass flux across the interface with time.

The average mass flux increases during the first 5s as the temperature increases at the interface due to Marangoni convection as compared to the case when it is not considered. The difference in both the cases after 1 min is approximately 2% which increases with the time eventually. Hence, we can say that the Marangoni convection influences the evaporation and it should be considered while doing any simulation to imitate the real situation.

Chapter 6

FUTURE WORK

The following future study can be conducted by referring to the present numerical model.

1. The numerical model can be extended to study the droplet evaporation with receding contact line i.e. depinning of the droplet.
2. A parametric study for different contact angles with the same volume can be done.
3. The effect of external air convection can be studied.
4. Droplet spreading on the substrate can be characterized.
5. The model can be extended to study thin-film evaporation.

- Thin-film Evaporation:

When a liquid wets a solid wall, the extended meniscus can be divided into 3 regions as shown in figure 6.1. The first region is the adsorbed region which has the uniform thickness. The adhesive forces are maximum in this region, this force arising due to the molecular attraction is also known as disjoining pressure. Thermal resistance is infinite in this region and so there is no evaporation from this region.

The second region is the thin-film region that is characterized by its curvature which is the maximum in this region as compared to the previous region because there is no curvature in it. The adhesive forces at the liquid-solid interface are strong while it decreases as we move up thus, the thermal resistance is minimum in this region resulting in maximum evaporation taking place at the curvature. The pressure due to the curvature which is known as capillary pressure is maximum in this region.

The third region is the bulk meniscus which has minimal adhesive forces less curvature and the range of thermal resistance is between the previously mentioned regions. The bulk region is responsible for feeding the liquid to the evaporating meniscus i.e. the thin-film region during the evaporation. The disjoining pressure decreases along the curvature of the adsorbed region to the bulk meniscus. Here, the capillary pressure is responsible for governing the shape of the transition or thin-film region while the flow of liquid is governed by the disjoining pressure. [16]

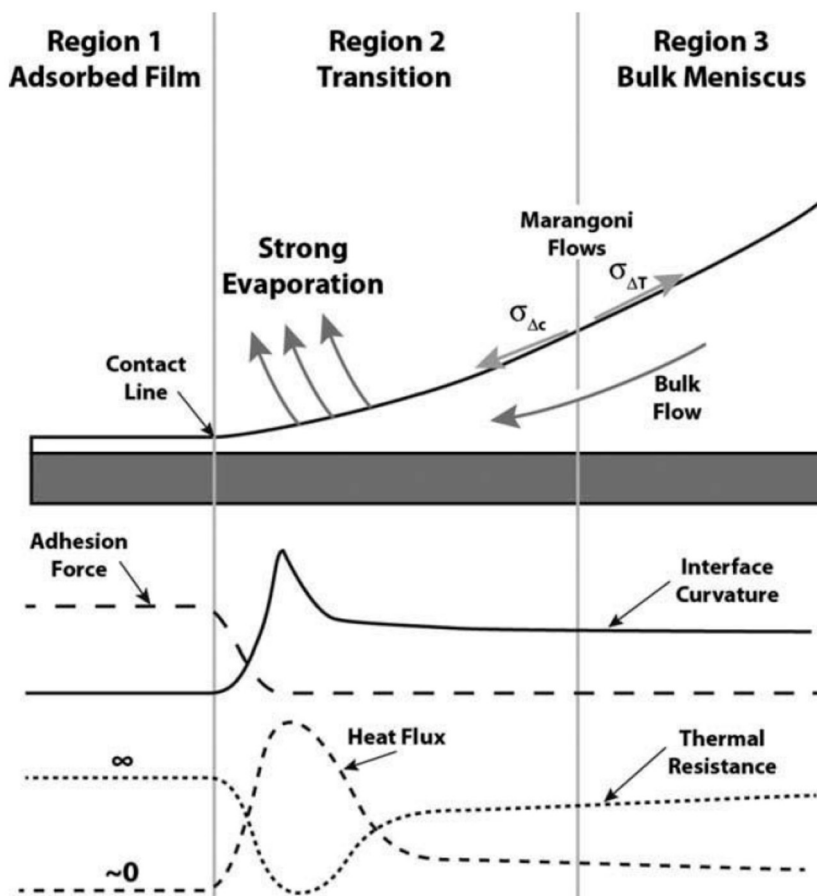


Figure 6.1 Division of the extended droplet meniscus.

References

- [1]. <https://www.slideshare.net/gavin40/thermal-physics-core>
- [2]. Berthier, Jean. Micro-drops and digital microfluidics. William Andrew, 2012.
- [3]. https://en.wikipedia.org/wiki/Eotvos_rule
- [4]. Hendarto, Erwin, and Yogesh B. Gianchandani. "Size sorting of floating spheres based on Marangoni forces in evaporating droplets." *Journal of Micromechanics and Microengineering*, 2013.
- [5]. Tam, Daniel, et al. "Marangoni convection in droplets on super hydrophobic surfaces." *Journal of Fluid Mechanics* 624, 2009.
- [6]. E. Olsson and G. Kreiss. A conservative level set method for two-phase flows. *Journal of Computational Physics*, 210(1), 2005.
- [7]. Peter Smereka and J.A. Sethian. Level set methods for fluid interfaces. *Annual review of Fluid Mechanics*, 2003.
- [8]. K. Yang, F. Hong, and P. Cheng, "A fully coupled numerical simulation of sessile droplet evaporation using Arbitrary Lagrangian-Eulerian formulation," *Int. J. Heat Mass Transf.*, vol. 70, 2014.
- [9]. Lars Olovsson, "Livermore Software Technology Corporation." U.S. Patent 7167816B1, issued 2007.
- [10]. G. Son, "A level-set method for analysis of microdroplet evaporation on a heated surface," *J. Mech. Sci. Technol.*, vol. 24, no. 4, 2010.
- [11]. <https://www.comsol.com/blogs/intro-to-modeling-evaporative-cooling>
- [12]. Equations are given in the ale module in COMSOL Multiphysics 5.3.
- [13]. <https://www.comsol.com/blogs/modeling-marangoni-convection-with-comsolmultiphysics>

- [14]. <https://www.comsol.com/multiphysics/marangoni-effect>
- [15]. Matin's experimental data for droplet evaporation on a glass substrate.
- [16]. Ojha, Manas, Arya Chatterjee, Frank Mont, E. F. Schubert, Peter C. Wayner, and Joel L. Plawsky. "The role of solid surface structure on dropwise phase change processes." *International Journal of Heat and Mass Transfer* 53, no. 5, 2010.

Biographical Information

Ritul Niravkumar Gandhi earned his bachelor degree in Mechanical Engineering from Gujarat Technological University, India, in 2015. He joined The University of Texas at Arlington in Spring 2016. He is currently a member of Integrated Micro-Nano fluidic systems laboratory at UTA. His area of research is in MEMS devices, thermal management in electronics and computational methods for fluids & heat transfer.